Nano-Micro Letters
e-ISSN 2150-5551
CN 31-2103/TB
CORRECTION
https://doi.org/10.1007/s40820-026-02239-z

Cite as
Nano-Micro Lett.
(2027) 19:6

Correction: Copper-Based Targeted Nanocatalytic Therapeutics for Non-Small Cell Lung Cancer

Yongfei Fan[1,3], Jiao Chang[2,3], Xichun Qin[1], Meng Li[2,3], Yan Li[2,3], Leilei Wu[4], Kun Li[1], Zhimin Chen[5], Yani Li[2,3], Zhongmin Tang[2,3] ✉, Dong Xie[1] ✉, Jianlin Shi[6]

Yongfei Fan and Jiao Chang have contributed equally to this work.

The original article can be found online at https://doi.org/10.1007/s40820-025-01998-5.

✉ Zhongmin Tang, zhongmintang@tongji.edu.cn; Dong Xie, xiedong@tongji.edu.cn
[1] Department of Thoracic Surgery, Shanghai Pulmonary Hospital, School of Medicine, Tongji University, Shanghai 200433, People's Republic of China
[2] Department of Radiology, Tongji Hospital, School of Medicine, Tongji University, Shanghai 200331, People's Republic of China
[3] Shanghai Frontiers Science Center of Nanocatalytic Medicine, School of Medicine, Tongji University, Shanghai 200331, People's Republic of China
[4] Department of Thoracic Surgery, Zhejiang Cancer Hospital, Hangzhou Institute of Medicine, Chinese Academy of Sciences, Hangzhou, Zhejiang 310022, People's Republic of China
[5] Department of Medical Oncology, Shanghai Pulmonary Hospital, School of Medicine, Tongji University, Shanghai 200433, People's Republic of China
[6] Shanghai Institute of Ceramics Chinese Academy of Sciences, Research Unit of Nanocatalytic Medicine in Specific Therapy for Serious Disease, Chinese Academy of Medical Sciences, Shanghai 200050, People's Republic of China

Correction to:
Nano-Micro Lett. (2026) 18:152.
https://doi.org/10.1007/s40820-025-01998-5

Following publication of the original article [1], the authors reported the article needed to be updated. The required corrections are detailed below.

1) The **full name of DMSA** was incorrectly written at its first occurrence in the **Highlights, Abstract, Introduction, Fig. 1 legend, and Supplementary Information (Section S1, Experimental Section)**. The correct expression is **"copper (Cu) and dimercaptosuccinic acid (DMSA)."**
2) The **chemical** equations **in the Table of Contents graphic (TOC) and Fig. 1** were incorrectly written. The correct expressions are "**$Cu^{+} + H_2O_2 \rightarrow Cu^{2+} + OH^{-} + \bullet OH$.**"
3) Due to an error during image assembly involving copy-and-paste operations, **the statistical plot for PC-9 in Fig. 6i was incorrectly duplicated from that of NCI-H1975.**

All the above corrections do not affect the final conclusions of the article. The correct Table of Contents graphic, Figs. 1 and 6 have been provided in this Correction. The Supplementary file has been updated as well.

Published online: 28 July 2026

The incorrect Table of Contents graphic is:

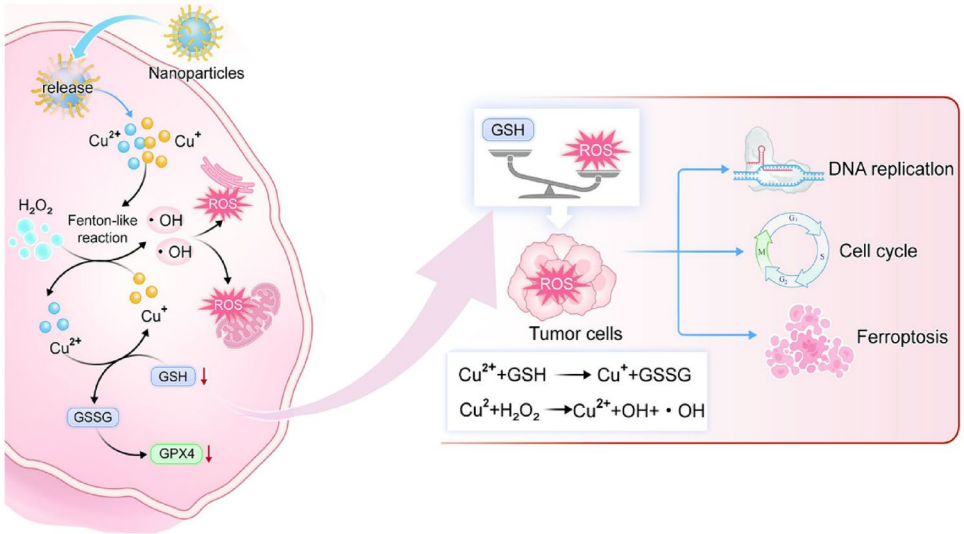

The correct Table of Contents graphic is:

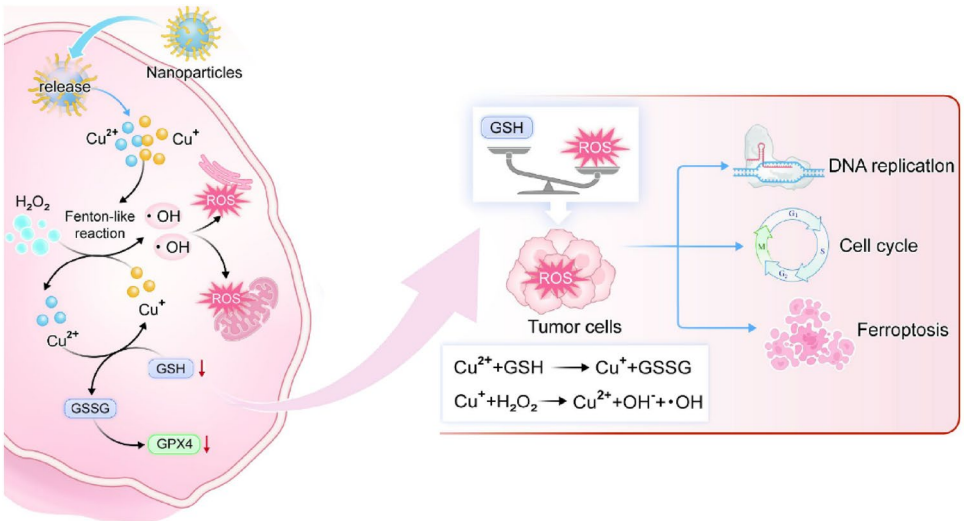

 https://doi.org/10.1007/s40820-026-02239-z

The incorrect Fig. 1 is:

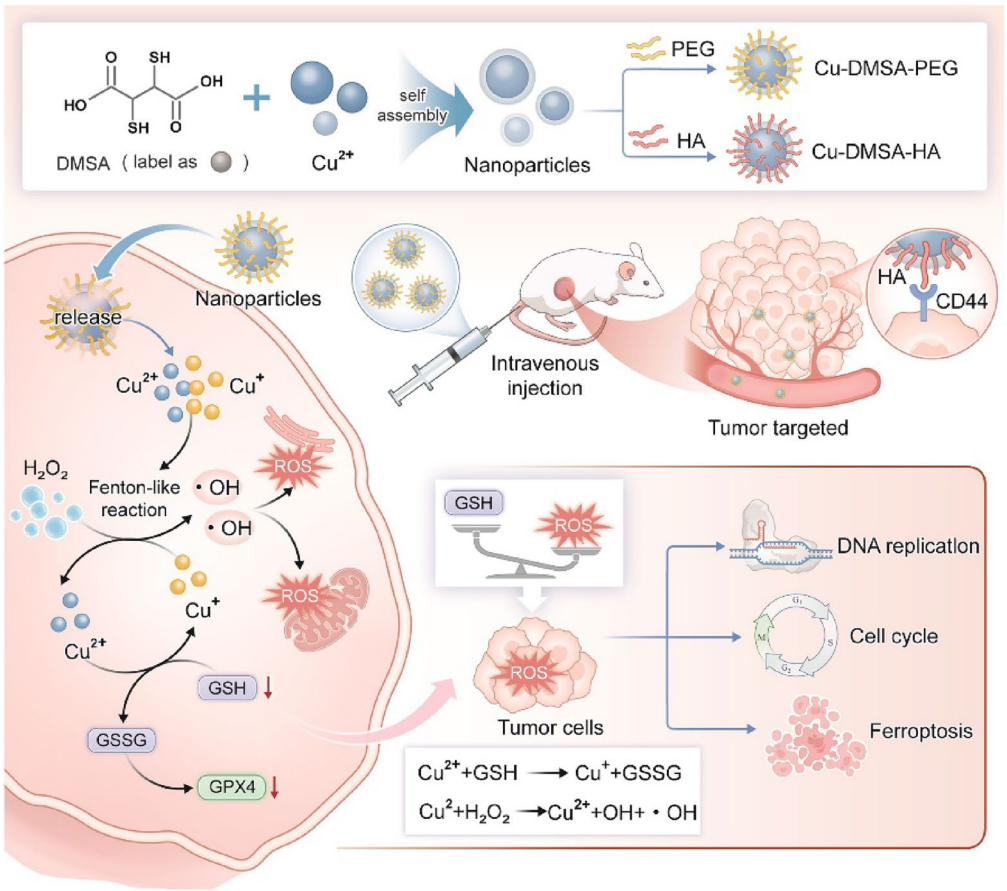

Fig. 1 Preparation schematics of nanoparticles (NPs) and proposed therapeutic mechanism. **a** Schematic illustration of the synthesis of copper–N,N-dimethyl-N-phenylsulfonylbisamine (DMSA) NPs modified with polyethylene glycol (Cu-DMSA-PEG NPs) and hyaluronic acid (HA) (Cu-DMSA-HA NPs), respectively. **b** Proposed biological mechanism of Cu-DMSA-HA-induced ferroptosis in tumor cells. Following cellular internalization, Cu-DMSA-HA NPs, which are assembled via coordination chemistry, catalyze intracellular reactive oxygen species (ROS) generation through glutathione (GSH)-mediated reduction and subsequent Fenton-like reactions. The resulting ROS accumulation triggers oxidative damage to mitochondria and the endoplasmic reticulum of tumor cells, leading to downregulation of glutathione peroxidase 4 (GPX4), a key regulator protecting against ferroptosis. **c** Mechanism of in vivo tumor targeting by Cu-DMSA-HA. Cu-DMSA-HA facilitates selective binding to cluster of differentiation 44 (CD44) receptors overexpressed on tumor cells, enhancing tumor-specific accumulation. **d** Antitumor mechanism of Cu-DMSA-HA in vivo. Cu-DMSA-HA inhibits tumor progression by suppressing DNA replication and cell cycle progression while inducing ferroptosis.

The correct Fig. 1 is:

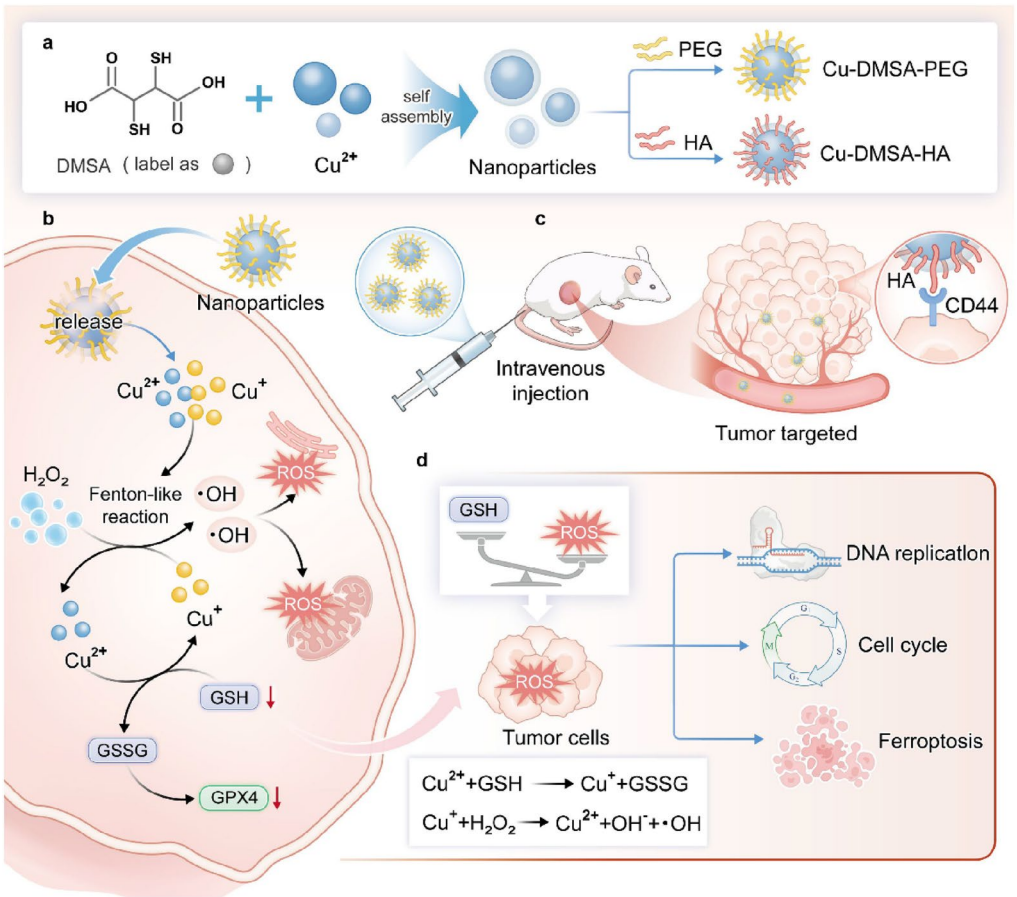

Fig. 1 Preparation schematics of nanoparticles (NPs) and proposed therapeutic mechanism. **a** Schematic illustration of the synthesis of copper—dimercaptosuccinic acid (DMSA) NPs modified with polyethylene glycol (Cu-DMSA-PEG NPs) and hyaluronic acid (HA) (Cu-DMSA-HA NPs), respectively. **b** Proposed biological mechanism of Cu-DMSA-HA-induced ferroptosis in tumor cells. Following cellular internalization, Cu-DMSA-HA NPs, which are assembled via coordination chemistry, catalyze intracellular reactive oxygen species (ROS) generation through glutathione (GSH)-mediated reduction and subsequent Fenton-like reactions. The resulting ROS accumulation triggers oxidative damage to mitochondria and the endoplasmic reticulum of tumor cells, leading to downregulation of glutathione peroxidase 4 (GPX4), a key regulator protecting against ferroptosis. **c** Mechanism of in vivo tumor targeting by Cu-DMSA-HA. Cu-DMSA-HA facilitates selective binding to cluster of differentiation 44 (CD44) receptors overexpressed on tumor cells, enhancing tumor-specific accumulation. **d** Antitumor mechanism of Cu-DMSA-HA in vivo. Cu-DMSA-HA inhibits tumor progression by suppressing DNA replication and cell cycle progression while inducing ferroptosis.

The incorrect Fig. 6 is:

Fig. 6 Evaluation of oxidative stress and ferroptosis induction by Cu-DMSA-HA in NSCLC cells. **a** ROS staining of PC-9 and NCI-H1975 cells following treatment with PBS, Cu-DMSA-PEG, or Cu-DMSA-HA. Scale bar: 100 μm. **b** Flow cytometry analysis of ROS levels in PC-9 and NCI-H1975 cells treated with PBS, Cu-DMSA-PEG, or Cu-DMSA-HA. **c** Mitochondrial membrane potential (Δψm) staining of PC-9 and NCI-H1975 cells following treatment with PBS, Cu-DMSA-PEG, or Cu-DMSA-HA, and **d** corresponding quantitative fluorescence intensity analyses (n = 3; mean ± SD). Oneway ANOVA followed by Tukey's post hoc test. Red fluorescence: JC-1 aggregates (healthy mitochondria, high membrane potential); green fluorescence: JC-1 monomers (damaged mitochondria, low membrane potential). Scale bar: 100 μm. **e** Flow cytometry analysis of Δψm in PC-9 and NCI-H1975 cells treated with PBS, Cu-DMSA-PEG, or Cu-DMSA-HA. **f** TEM images depicting ultrastructural changes in PC-9 and NCI-H1975 cells after treatment with PBS, Cu-DMSA-PEG, or Cu-DMSA-HA. N: nucleus; M: mitochondria; ER: endoplasmic reticulum; ASS: autolysosome. **g** Quantification of reduced GSH and GSSG levels in PC-9 and NCI-H1975 cells following treatments with PBS, Cu-DMSA-PEG, or Cu-DMSAHA (n = 3; mean ± SD). Oneway ANOVA followed by Tukey's post hoc test. **h** Western blot analysis and **i** quantification of GPX4 protein expression in PC-9 and NCI-H1975 cells after treatments with PBS, Cu-DMSA-PEG, or Cu-DMSA-HA (n = 3; mean ± SD). Oneway ANOVA followed by Tukey's post hoc test. C11-BODIPY staining and fluorescence microscopy analysis of lipid ROS accumulation in **j-k** PC-9 and **m–n** NCI H1975 cells after treatments with PBS, Cu-DMSA-PEG, Cu-DMSA-HA, DMSO, Cu-DMSA–PEG + ferrostatin-1 (Fer-1), or Cu-DMSA-HA + Fer-1 (n = 3; mean ± SD). Oneway ANOVA followed by Tukey's post hoc test. C11-BODIPY staining flow cytometry quantification of lipid ROS levels in l PC-9 and **o** NCI H1975 cells after treatments with PBS, Cu-DMSA-PEG, Cu-DMSA-HA, DMSO, Cu-DMSA-PEG + Fer-1, or Cu-DMSAHA + Fer-1. CCK-8 assay of cell viability in **p** PC-9 and **q** NCIH1975 cells after treatments with DMSO, Cu-DMSA-PEG, Cu-DMSA-HA, or in combination with Fer-1 (n = 4; mean ± SD). Oneway ANOVA followed by Tukey's post hoc test. *$P < 0.05$; **$P < 0.01$; ***$P < 0.001$; ****$P < 0.0001$.

https://doi.org/10.1007/s40820-026-02239-z

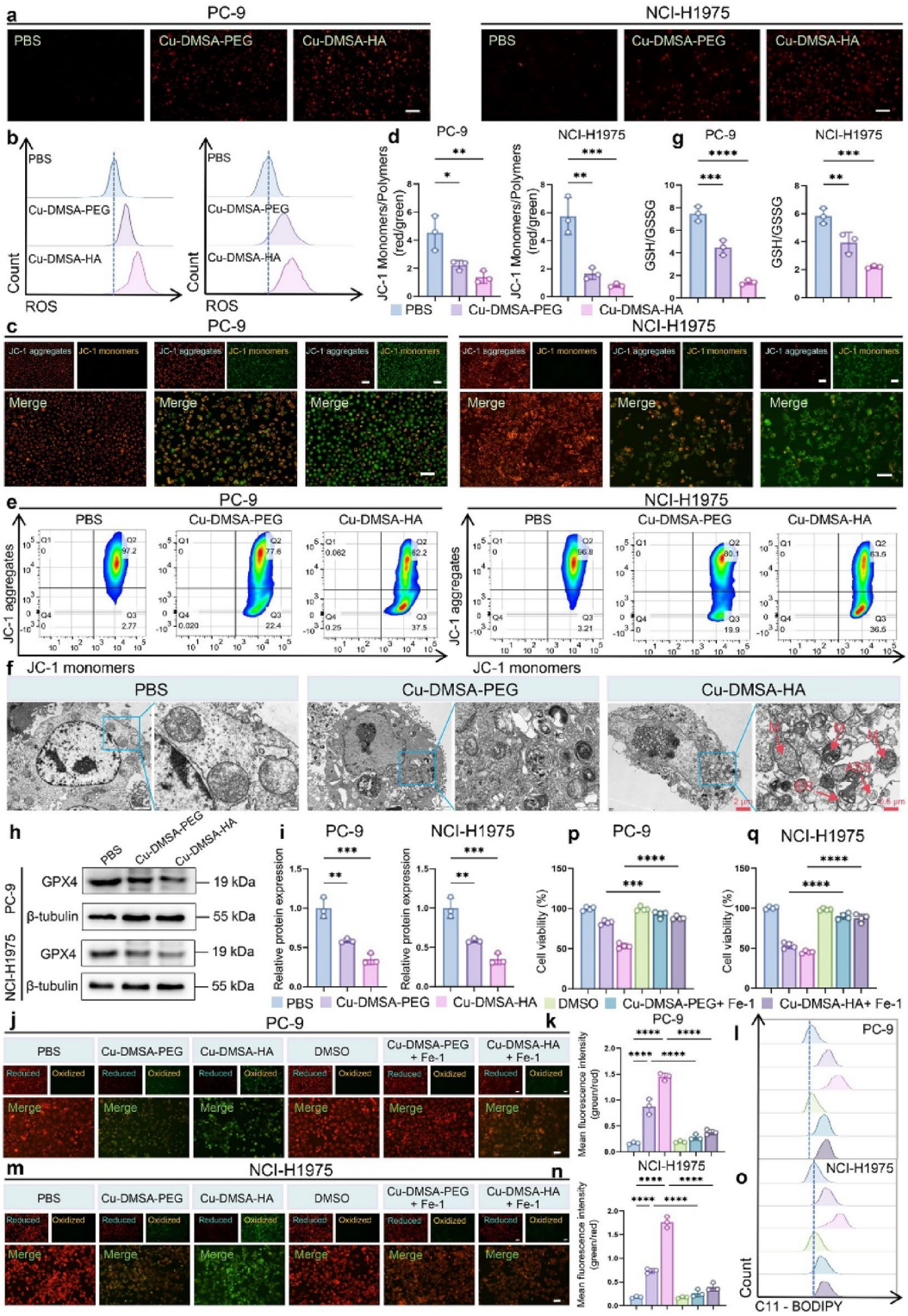
a
PC-9
NCI-H1975
PBS
Cu-DMSA-PEG
Cu-DMSA-HA
b
Count
ROS
d
JC-1 Monomers/Polymers (red/green)
g
GSH/GSSG
c
JC-1 aggregates
JC-1 monomers
Merge
e
JC-1 aggregates
JC-1 monomers
f
h
GPX4
β-tubulin
19 kDa
55 kDa
i
Relative protein expression
p
q
Cell viability (%)
DMSO
Cu-DMSA-PEG+ Fe-1
Cu-DMSA-HA+ Fe-1
j
k
Mean fluorescence intensity (green/red)
l
o
C11 - BODIPY
m
n

The correct Fig. 6 is:

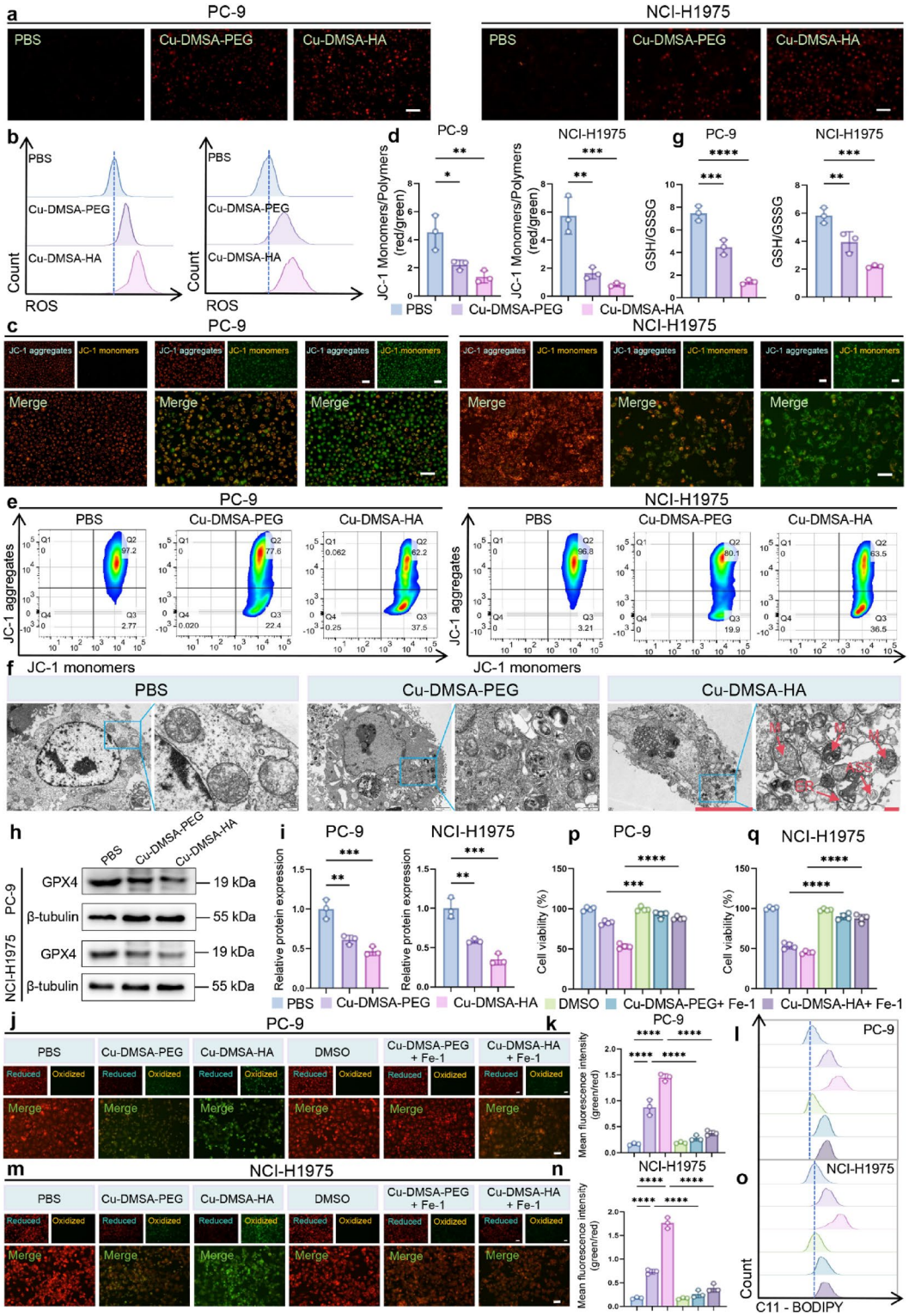

◂**Fig. 6** Evaluation of oxidative stress and ferroptosis induction by Cu-DMSA-HA in NSCLC cells. **a** ROS staining of PC-9 and NCI-H1975 cells following treatment with PBS, Cu-DMSA-PEG, or Cu-DMSA-HA. Scale bar: 100 μm. **b** Flow cytometry analysis of ROS levels in PC-9 and NCI-H1975 cells treated with PBS, Cu-DMSA-PEG, or Cu-DMSA-HA. **c** Mitochondrial membrane potential (Δψm) staining of PC-9 and NCI-H1975 cells following treatment with PBS, Cu-DMSA-PEG, or Cu-DMSA-HA, and **d** corresponding quantitative fluorescence intensity analyses (n = 3; mean ± SD). Oneway ANOVA followed by Tukey's post hoc test. Red fluorescence: JC-1 aggregates (healthy mitochondria, high membrane potential); green fluorescence: JC-1 monomers (damaged mitochondria, low membrane potential). Scale bar: 100 μm. **e** Flow cytometry analysis of Δψm in PC-9 and NCI-H1975 cells treated with PBS, Cu-DMSA-PEG, or Cu-DMSA-HA. **f** TEM images depicting ultrastructural changes in PC-9 and NCI-H1975 cells after treatment with PBS, Cu-DMSA-PEG, or Cu-DMSA-HA. N: nucleus; M: mitochondria; ER: endoplasmic reticulum; ASS: autolysosome. **g** Quantification of reduced GSH and GSSG levels in PC-9 and NCI-H1975 cells following treatments with PBS, Cu-DMSA-PEG, or Cu-DMSAHA (n = 3; mean ± SD). Oneway ANOVA followed by Tukey's post hoc test. **h** Western blot analysis and **i** quantification of GPX4 protein expression in PC-9 and NCI-H1975 cells after treatments with PBS, Cu-DMSA-PEG, or Cu-DMSA-HA (n = 3; mean ± SD). Oneway ANOVA followed by Tukey's post hoc test. C11-BODIPY staining and fluorescence microscopy analysis of lipid ROS accumulation in **j-k** PC-9 and **m–n** NCI-H1975 cells after treatments with PBS, Cu-DMSA-PEG, Cu-DMSA-HA, DMSO, Cu-DMSA–PEG + ferrostatin-1 (Fer-1), or Cu-DMSA-HA + Fer-1 (n = 3; mean ± SD). Oneway ANOVA followed by Tukey's post hoc test. C11-BODIPY staining flow cytometry quantification of lipid ROS levels in l PC-9 and **o** NCI-H1975 cells after treatments with PBS, Cu-DMSA-PEG, Cu-DMSA-HA, DMSO, Cu-DMSA-PEG + Fer-1, or Cu-DMSAHA + Fer-1. CCK-8 assay of cell viability in **p** PC-9 and **q** NCIH1975 cells after treatments with DMSO, Cu-DMSA-PEG, Cu-DMSA-HA, or in combination with Fer-1 (n = 4; mean ± SD). Oneway ANOVA followed by Tukey's post hoc test. $^{*}P < 0.05$; $^{**}P < 0.01$; $^{***}P < 0.001$; $^{****}P < 0.0001$.

The original article [1] has been corrected.

Reference

1. Y. Fan, J. Chang, X. Qin et al., Copper-based targeted nanocatalytic therapeutics for non-small cell lung cancer. Nano-Micro Lett. **18**, 152 (2026). https://doi.org/10.1007/s40820-025-01998-5